Geol. Soc. Malaysia, Bulletin 41, December 1997; pp. 151–158

Cumulative dip plot method

SAHAT SADIKUN

School of Science & Technology
Universiti Malaysia Sabah
Locked Bag 2073
88999 Kota Kinabalu
Sabah

Abstract: It is usual for a well to encounter faults, unconformities and sequence boundaries along its depth. Identification of these features based on the scatter of the 'tadpoles' from the diplog data alone may be difficult. To assist this identification, a cumulative dip plot, a crossplot of bedding plane orientation against depth was used. This method involves plotting the cumulative bedding plane dip with their appropriate dip directions against depth. The dip directions were colour coded into four compass quadrants: north-east (0–90°), east-south (90–180°), south-west (180–270°) and west-north (270–360°). A simple layer cake bedding will produce a straight line and a single colour cumulative plot. It is usual for bedding dips magnitude and directions or both to change when passing through a fault or unconformity, and thus will be represented by points of inflection (discontinuity and perhaps change of colours). In this study, diplog data from two wells (Well A and B) in the Baram Delta Field was used in plotting two cumulative dip plots. Results were compared with the previously interpreted faults, unconformities and horizons (sedimentary cycle boundaries) based on other wireline log data (sonic, resistivity and gamma) and seismic data. Results of the two cumulative dip plots seem to be in agreement with the previous results. This method proves to be a useful supplement study especially in structurally complex areas.

INTRODUCTION

In the conventional method, the manner of the tadpole dips distribution in a dipmeter log can be classified into four patterns (Figs. 1 and 2). The green pattern represents constant dip and azimuth with depth, and is usually associated with a typical of thick shale sequence. In the red pattern the azimuth remains uniform but the angle of dip decreases upwards. Channel sands are usually associated with this motif that can be used also to determine the trend of sand body. The blue pattern shows uniform azimuth but an upward increase in the amount of dip. It shows prograding features such as delta fronts, submarine fans and sand bars. The final pattern, the random pattern represents erratic azimuths and dips angles. Massive beds lacking coherent bedding planes or slumped sands may be responsible for such a response. It may also result from tool malfunction or poor borehole conditions. The absence of computer dips is usually due to the dipmeter response to massive sandstones. Because there is no stratification, the dipmeter reads no change in resistivity so no dips can be computed.

There are possibilities of change in the dip magnitude, direction or both of a bedding plane in passing through faults, unconformities and sequence boundaries. However, unconformities and faults are not the only causes of these changes. Other causes include crossbedded sandstones encased in shales and siltstones, reefal carbonates in which no bedding planes are apparent, soft-sediment deformation, and chaotic bedding in turbidite deposits (Hurley, 1994). It should be emphasised that many structural and sedimentary features produce similar dipmeter log motifs which may be difficult to distinguish between them. A reliable interpretation therefore depends on a broad knowledge of local and regional geology and the availability of other well logs data taken in the same well or its vicinity as well as seismic data.

Faults, unconformities and sequence boundaries (sedimentary cycle boundaries) were usually determined using seismic data and tied with wireline logs found in the vicinity. Interpretation proved difficult in single well studies where no correlative logs are available.

CUMULATIVE DIP PLOTS

Many researchers have described the use of dipmeter in interpretations of structural dip, depositional environments, and fracture orientations (e.g. Gilreath, 1987; Adam *et al.,* 1987; Brenson, 1991; Pacht *et al.* , 1992; Bischke, 1994).

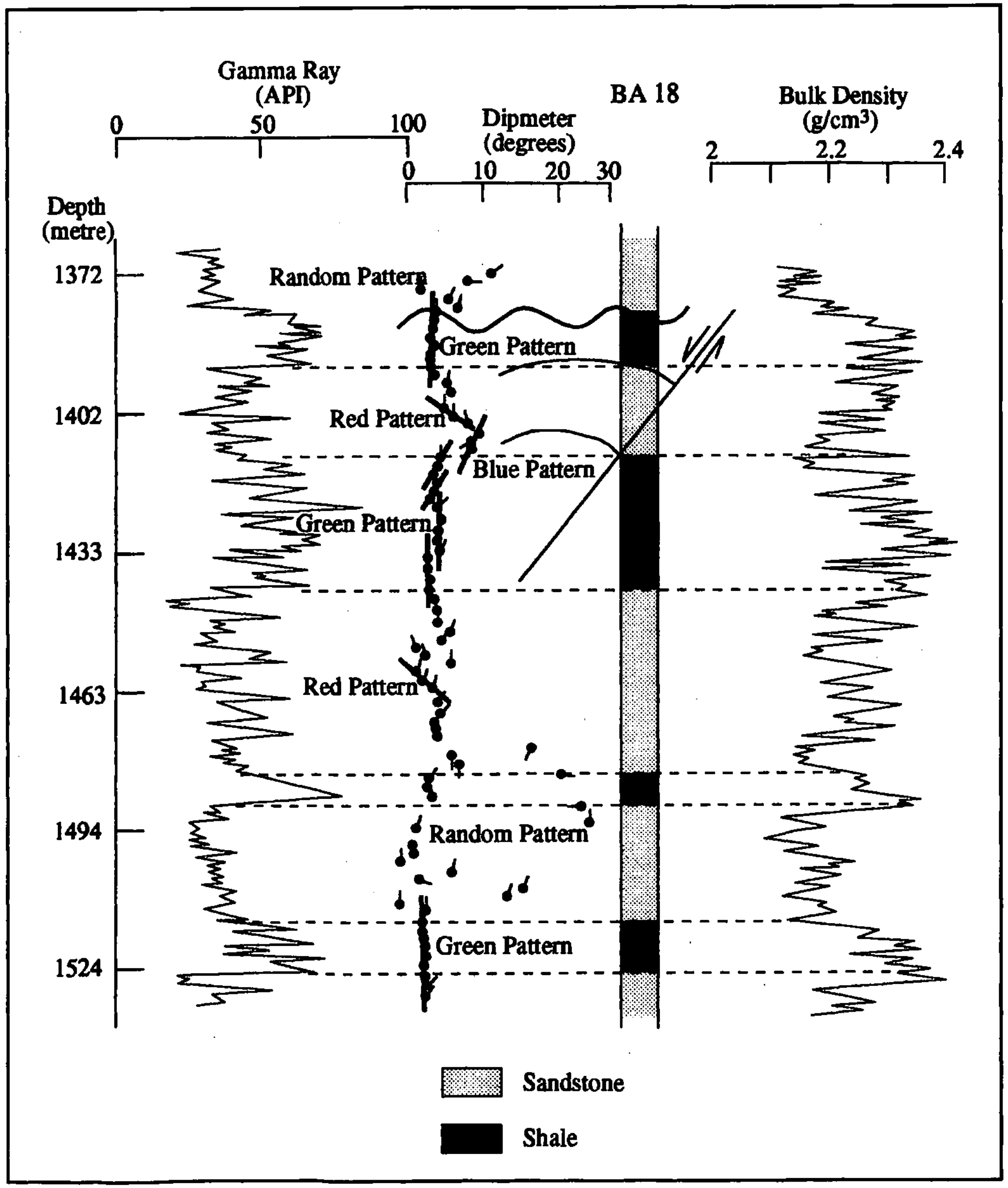

Figure 1. A growth fault producing a roll over in Well BA 18 (in the vicinity of the study area) at depth of 1,424 m (Lower Pliocene) dipping towards south west. Figure also shows several dip patterns.

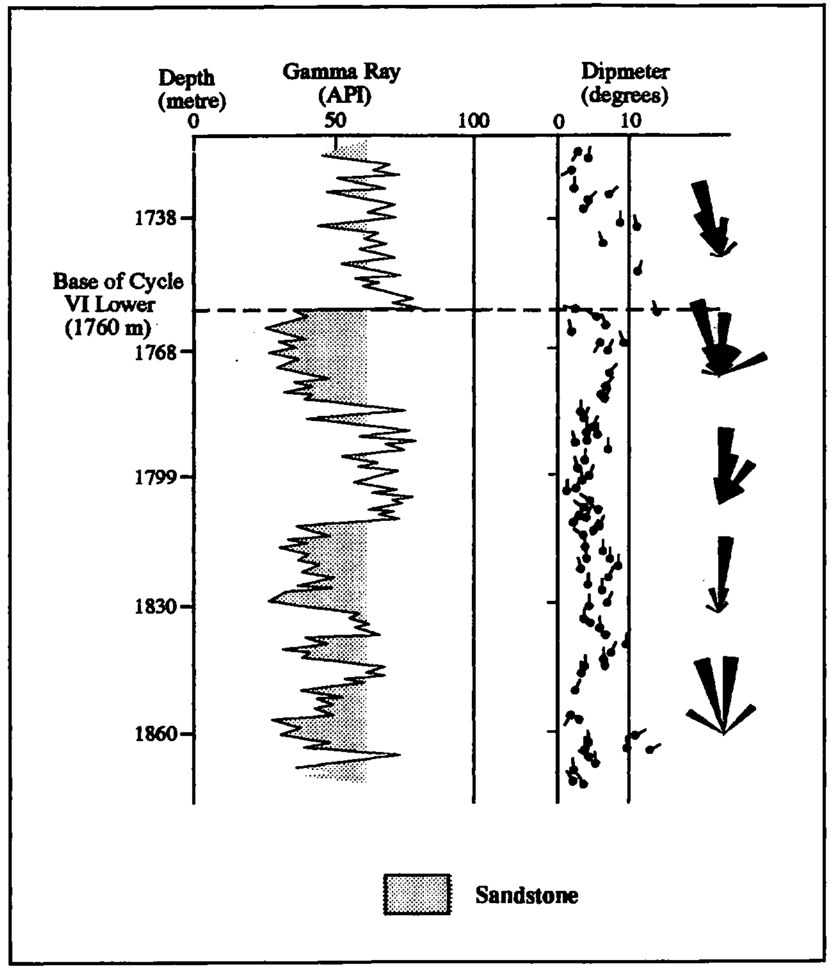

Figure 2. An example of gamma ray and dipmeter logs of Well B showing the base of Cycle VI Lower (Lower Pliocene).

In this study cumulative dip plot method (Hurley, 1994) was used in recognizing faults, unconformities and sequence boundaries (sedimentary cycles). The technique involves cross plotting cumulative bedding-plane dip against either depth or an arbitrary bedding-plane number that is a function of depth. For each successive sample number, the dip magnitude of the next depth is added to the cumulative dip of all shallower observations. In the cross plot, depths are arranged on the 'Y' axis from the shallowest at the top to the deepest at the bottom. Cumulative dips are plotted on the 'X' axis ranging from the minimum to the highest cumulative values. A simple constant layer cake bedding will give a smooth straight line plot.

Cumulative dip plots are not always straight lines. This happens because many oil wells were not drilled in structurally simple areas. The presence of inflection points on the cumulative cross plots is the basis of the interpretation process. They might suggest the presence of faults, unconformities or sequence boundaries. Cumulative cross plots provide clearer picture for interpretation than the conventional method (tadpole diagram) because they highlight subtle changes and average out an erratic pattern of the dip readings.

Table 1. Sample spreadsheet showing cumulative dip calculations of Well A.

Sample Number	Depth (metres)	Dip Magnitude (degrees)	Dip Direction (degrees)	Cumulative Dip (degrees)
1	272.56	2	45	2
2	273.78	7	325	9
3	276.83	5	300	14
4	279.57	10	1	24
5	280.18	25	335	49
6	292.07	19	300	68
7	292.68	8	225	76
8	320.12	7.5	180	83.5
9	323.17	1.8	115	85.3
10	325.61	4.5	120	89.8
11	325.91	6.3	170	96.1
12	326.22	7.8	34	103.9
13	328.05	8.3	70	112.2
14	328.66	6.4	160	118.6
15	330.79	4.2	52	122.8
16	330.18	6.3	260	129.1
17	335.37	6.4	75	135.5
18	337.80	7.7	65	143.2
19	348.48	8.3	105	151.5
20	366.77	20.6	15	172.1
21	375.00	11.7	80	183.8
22	375.30	9.2	20	193
23	377.44	3.7	210	196.7
24	384.76	17.6	258	214.3
25	385.06	17.6	205	231.9
26	387.50	7.6	177	239.5
27	389.63	1.7	287	241.2
28	403.35	1.7	285	242.9
29	409.15	7.8	10	250.7
30	419.82	5.7	340	256.4

METHOD

Dipmeter data from two wells of the Baram Delta Field (Wells A and B) were used in this study. The dipmeter data (tadpole diagrams) of these two wells were digitised (or using data from ASCII file) so that each 'tadpole' has the record of depth, bedding-plane dip and dip direction. For each successive depth, the bedding-plane dip magnitude of the next depth is added to the cumulative bedding-plane dip of all shallower observations. Commercial spreadsheet softwares such as EXCEL or Lotus 123 can be used in processing of data and plotting colour graphs. These cumulative bedding-plane dip readings are colour coded (not related to colours of tadpoles patterns described earlier) into compass quadrants: north-east (0–90°), east-south (90–180°), south-west (180–270°) and west-north (270–360°) based on their dip directions. A sample spreadsheet showing cumulative dip calculations from well A is shown in Table 1. A cross plot of cumulative bedding-plane dip against depth was then plotted for each well.

RESULTS OF CUMULATIVE DIP PLOTS

Cumulative dip plots of the two wells are shown in Figures 3 and 4. Results were compared to previously determined faults, unconformities and sequence boundaries. The plots clearly confirm the previous results and show improvement in the detection of these faults, unconformities and sequence boundaries.

Figure 3 represents a cumulative dip plot for Well A from Upper Miocene to Recent. A normal fault at 320 m depth was apparent in the Upper Pliocene sandstone beds (Fig. 5). There was a change of dip direction from south (170°) to northeast (34°) with a change of dip magnitude of only 1°. The base of Cycle VII at 488 m depth is in the shale bed (Fig. 5) showing a sudden change in dip direction from northwest (283°) to southeast (104°) without a change in the dip magnitude. The base of Cycle VI Upper at a depth of 813 m, is a boundary between shale and a blocky sandstone beds probably a channel (Fig. 6). It was represented by a change of dip direction from southeast (106°)

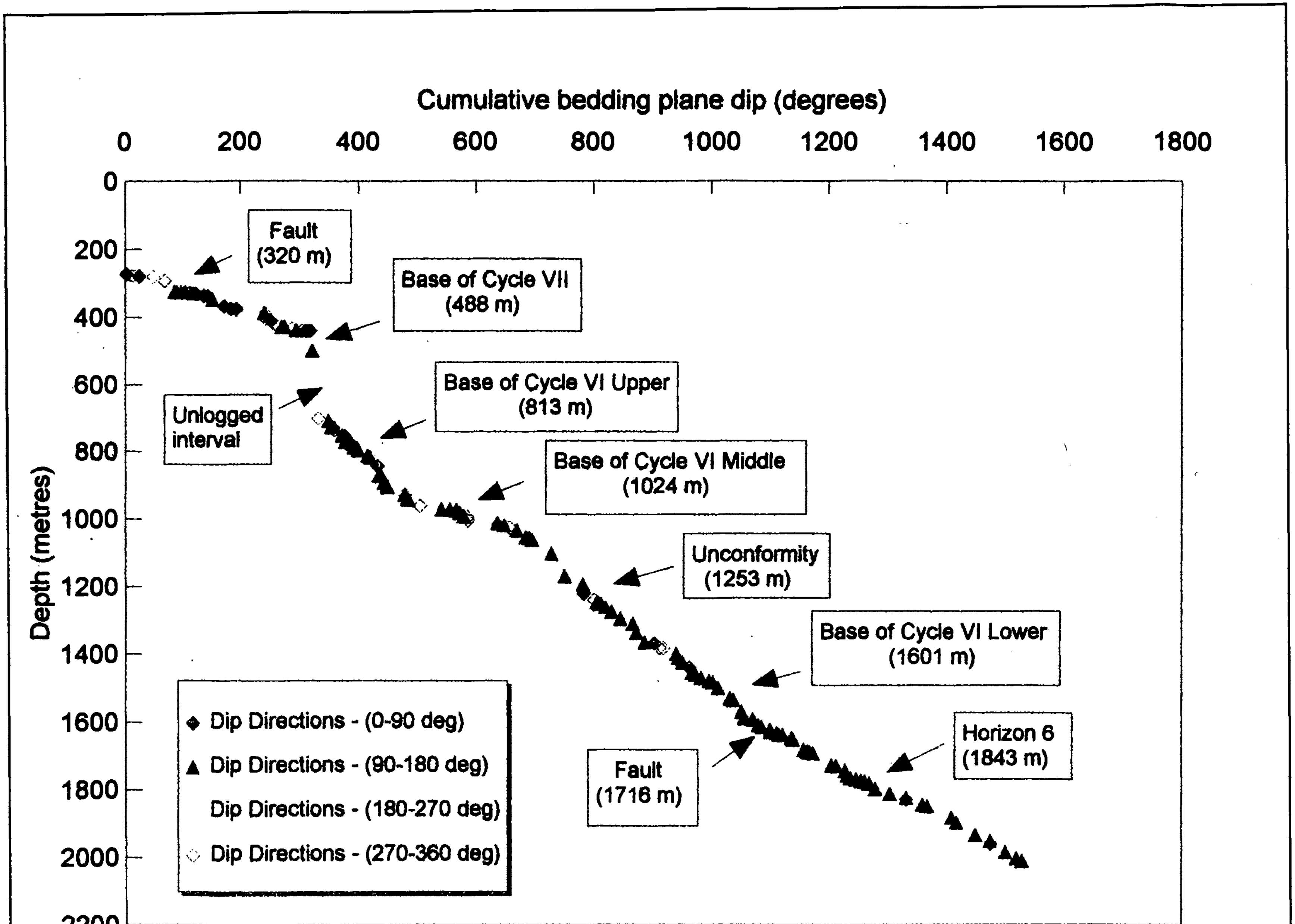

Figure 3 Cumulative dip plot for Upper Miocene to Recent sequence of Well A

Figure 3. Cumulative dip plot for Upper Miocene to Recent sequence of Well A.

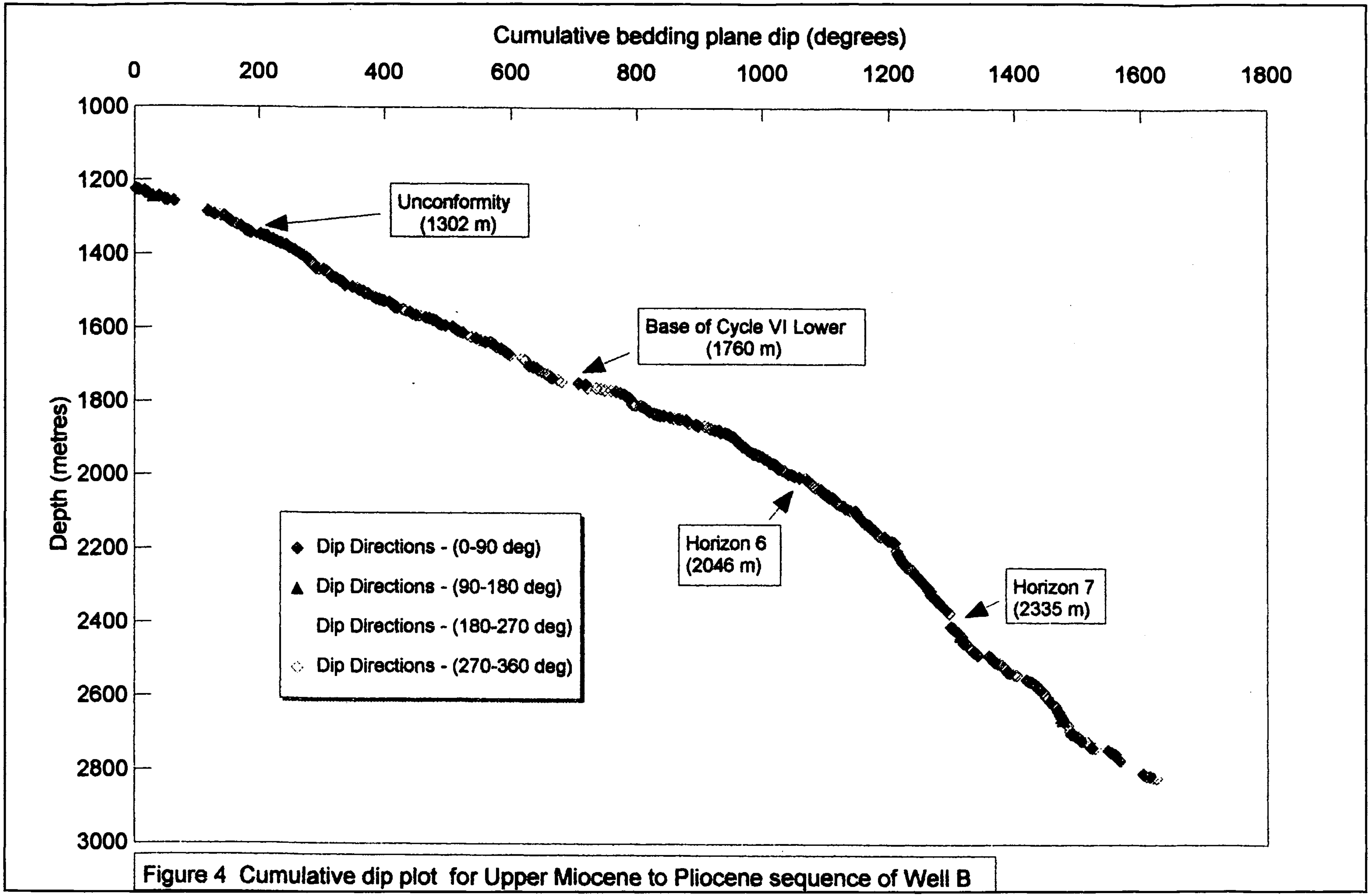

Figure 4. Cumulative dip plot for Upper Miocene to Recent sequence of Well B.

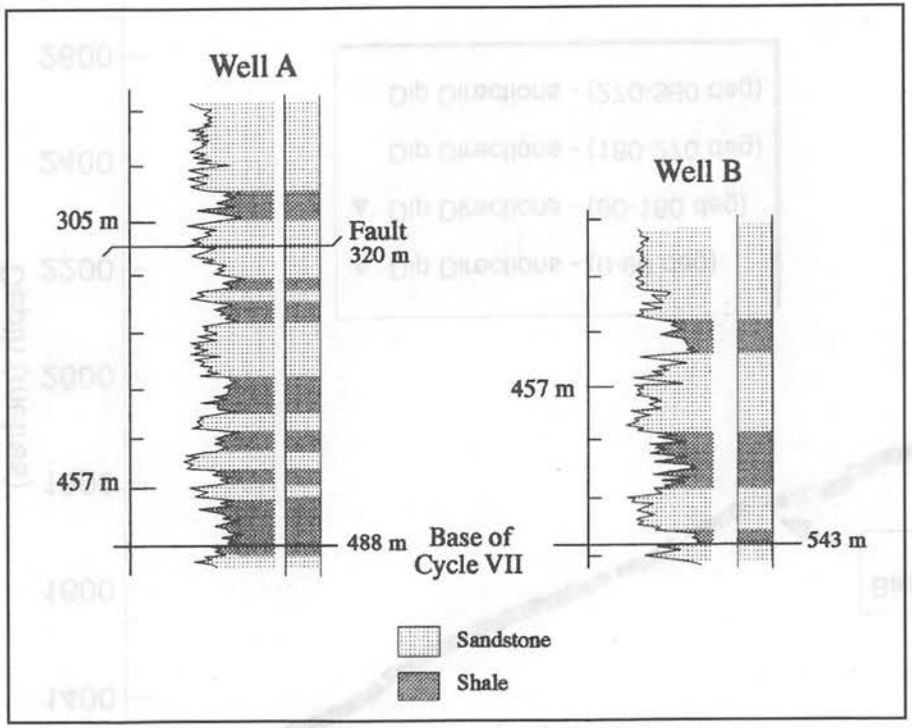

Figure 5. Stratigraphic interpretation of Cycle VII (Upper Pliocene) in Well A and Well B based on gamma ray log.

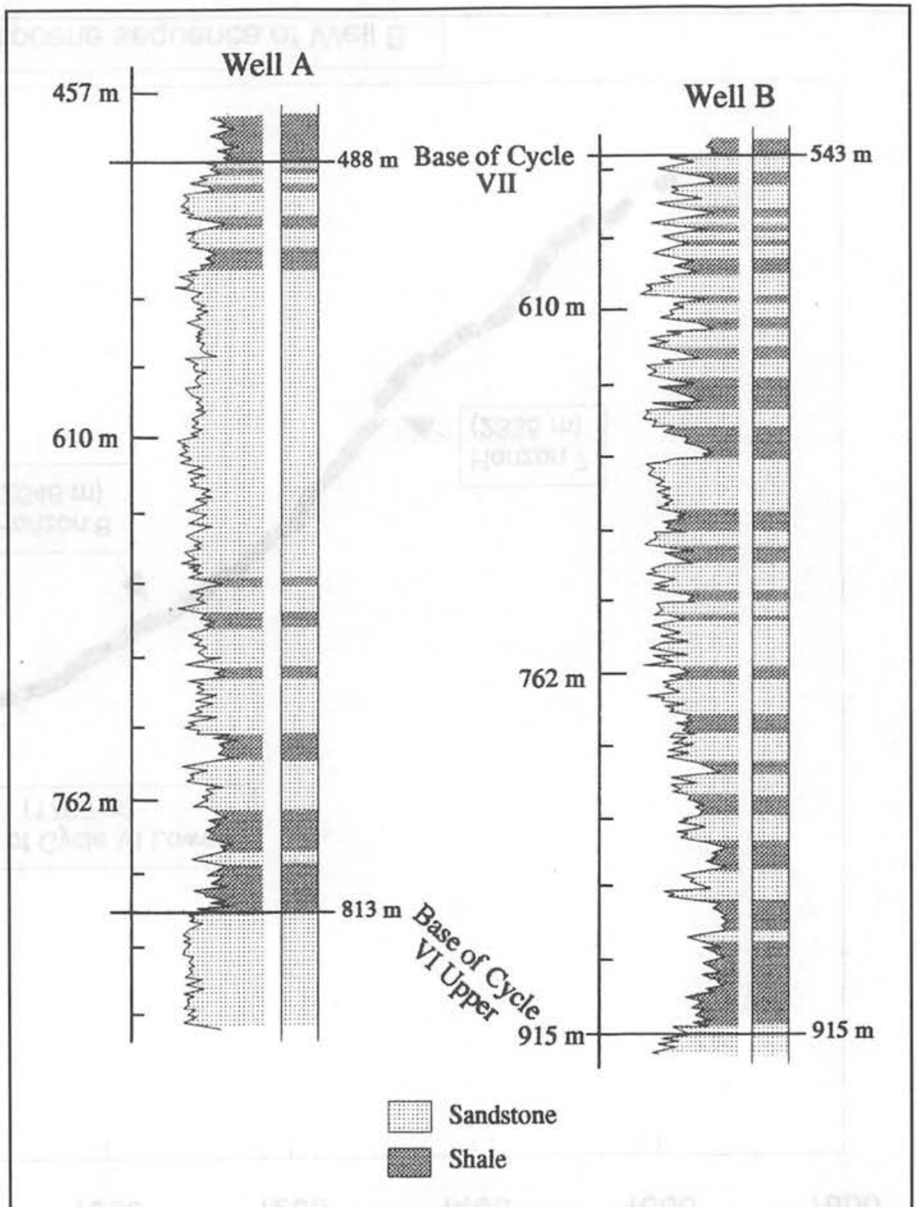

Figure 6. Stratigraphic interpretation of Cycle VII and Cycle VI Upper (Upper Pliocene) in Well A and Well B based on gamma ray log.

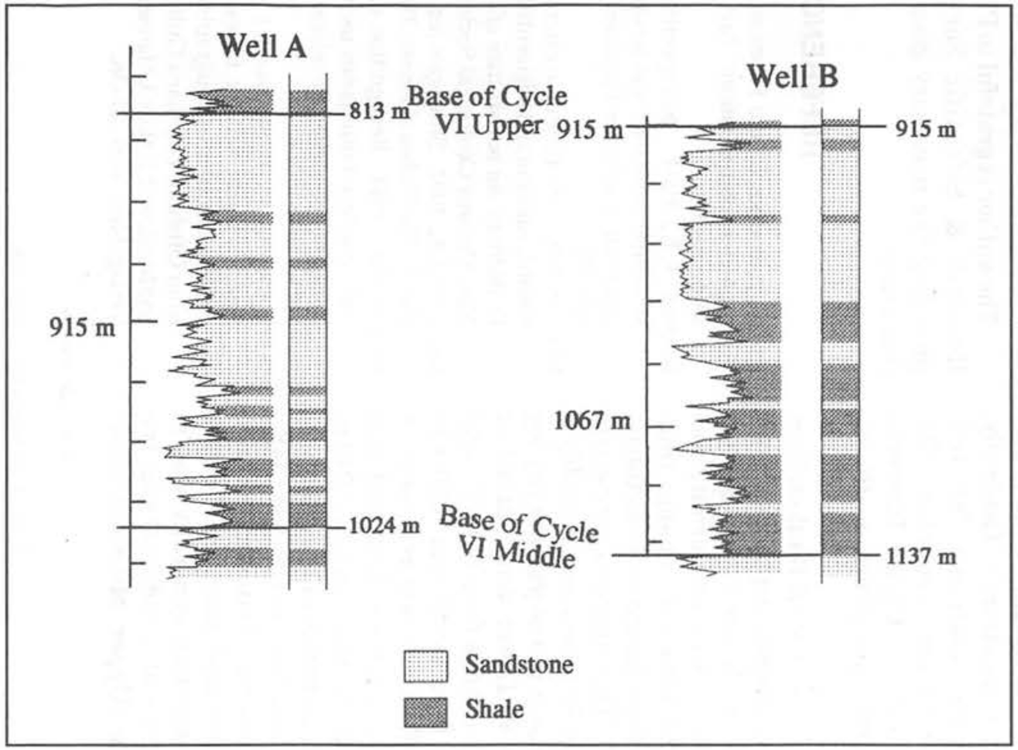

Figure 7. Stratigraphic interpretation of Cycle VI Upper and Cycle VI Middle (Lower Pliocene) in Well A and Well B based on gamma ray log.

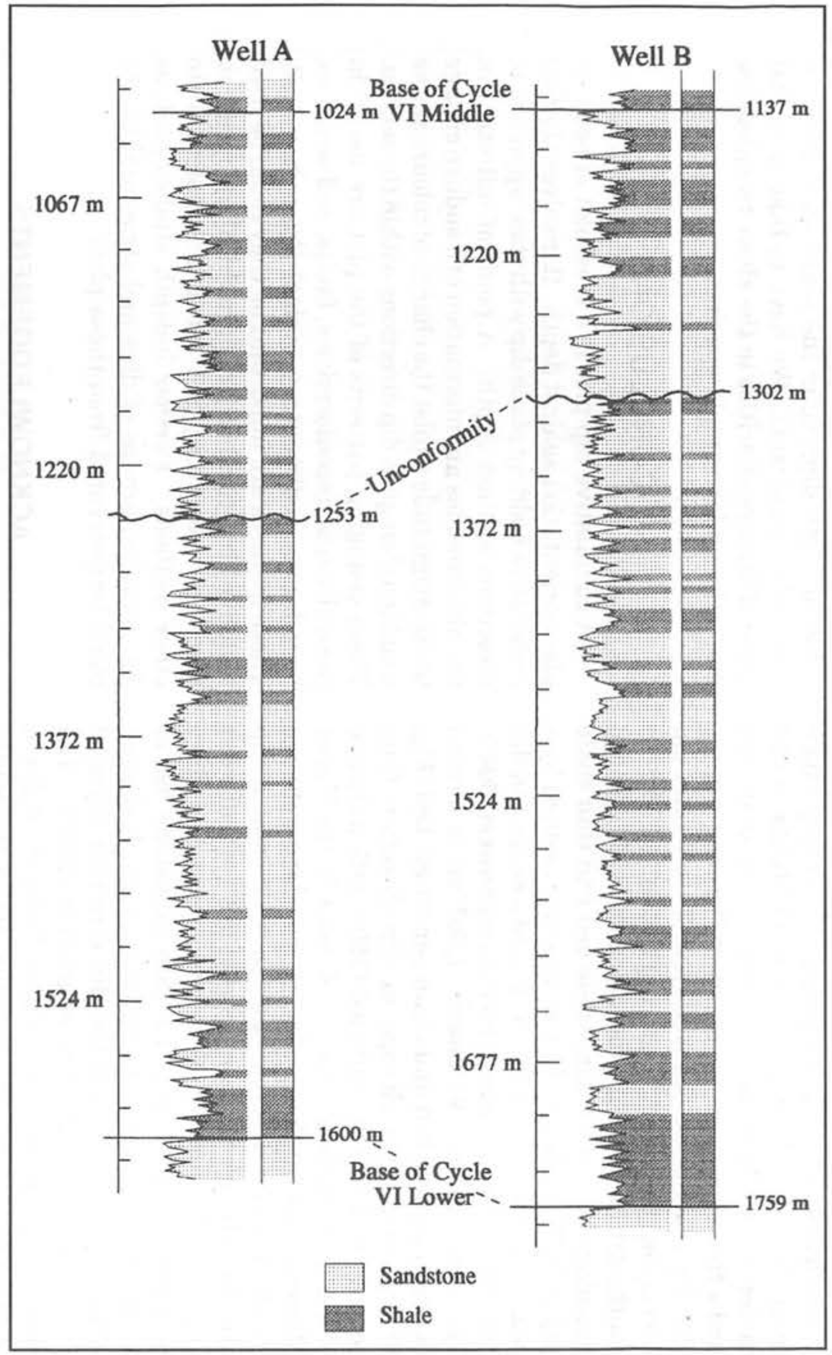

Figure 8. Stratigraphic interpretation of Cycle VI Middle and Cycle VI Lower (Lower Pliocene) in Well A and Well B based on gamma ray log.

to northwest (328°) and a change in dip magnitude from 16° to 3°. The base of Cycle VI Middle (1,024 m depth) is a boundary between a thin shale bed and a thin sandstone bed of Lower Pliocene (Fig. 7). The dip magnitude changed from 3° to 9° and dip direction changed from northwest (273°) to southwest (205°). An unconformity with a sharp boundary between a sandstone bed and thin shale bed at 1,253 m depth (Fig. 8) was represented by a change of dip from 1.8° to 16.1° and a change in dip direction from southwest (203°) to northwest (304°). The base of Cycle VI Lower (1,601 m) is located between a shale bed and clean sandstone bed (Fig. 8) representing a change in dip direction from southwest (210°) to southeast (160°) with a change of dip magnitude of only 1°. A fault in the Upper Miocene shale at depth of 1,716 m caused a change in dip magnitude from 4.6° to 18.7° and a dip direction change from southwest (192°) to southeast (135°). The horizon 6, represents a boundary between a shale bed and a thin sandstone bed of Upper Miocene age at a depth of 1,843 m. It showed a dip change of 2° and the dip direction changed from southeast (151°) to southwest (223°). The older sedimentary cycles (Upper Miocene) at depth of more than 1,900 m generally dip in the south-west directions (180°–270° quadrant). Generally, the dip direction was in the south-east (90°–180° quadrant) for the Lower Pliocene sequence. The youngest sedimentary cycles (Upper Pliocene) generally dip in the north-east direction (0°–90° quadrant).

Figure 4 represents data of Well B taken from a depth of 1,200 m to about 2,900 m depth (shallower data was not available) with age covering from Upper Miocene to Pliocene. An unconformity was detected at 1,302 m depth with a dip change from 4° to 9.8° and a dip direction change from northeast (22°) to northwest (290°). This unconformity exists between a thick clean sandstone layer probably a channel and shale as shown in the gamma ray log (Fig. 8). Base of Cycle VI Lower was marked at 1,760 m depth with a dip change from 6° to 27° and a dip direction change from northwest (330°) to northeast (43°). This inflection point represents a sharp base boundary between thick shale and thin regressive sandstone (Fig. 8). Horizon 6 at 2,046 m depth was detected with a change of dip of only 1° and change of dip direction from northwest (348°) to northeast (33°). It represents a boundary between a thin shale bed and a thin sandstone bed of Upper Miocene age. The dip direction generally was in the north-east direction (0°–90° quadrant) with the older sedimentary cycle (Upper Miocene) about 2,800 m depth dipping in the south-west direction (180°–270° quadrant). We have to take note that some of the irregularities in the above two plots are due to irregular sample spacing.

CONCLUSIONS

A cumulative dip plot is a crossplot of bedding plane orientation against depth. It involves plotting cumulative bedding plane dip with their appropriate directions against depth. A point of inflection in the plot provides an information of a sudden change in dip magnitude whilst the change of colours shows a sudden change in dip directions within the section. These changing patterns of the plot are useful in recognition of unconformities, faults, and sequence boundaries (sedimentary cycles) through a well. These features are important as they could be used to define structural or stratigraphical hydrocarbon traps in a reservoir, and act as a supplement to other methods. Further indepth studies such as dip domains, groups of dips and structural blocks could be generated from these plots.

ACKNOWLEDGEMENTS

The author is grateful to PETRONAS Petroleum Research & Scientific Services Sdn. Bhd. for providing the necessary geophysical data used in this study.

REFERENCES

ADAMS, J., BOURKE, L. AND FRISINGER, R., 1987. Strategies for dipmeter interpretation: Part 2. *The Technical Review* 35(4), 20–31.

BISCHKE, R.E., 1994. Interpreting sedimentary growth structures from well and seismic data (with examples). *American Association Petroleum Geologists Bulletin* 78(6), 873–892.

BRANSON, R.B., 1991. Productive trend and production history, South Louisiana and adjacent offshore. *In*: Goldthwaite, D. (Editor), *An introduction of central Gulf Coast geology*. New Orleans Geological Society, 61–70.

GILREATH, J.A., 1987. Strategies for dipmeter interpretation: part 1. *The Technical Review* 35(3), 28–41.

HURLEY, N.F., 1994. Recognition of faults, unconformities, and sequence boundaries using cumulative dip plots. *American Association Petroleum Geologists Bulletin* 78(8), 1173–1185.

PACHT, J.A., BOWEN, B., SHAFFER, B.L. AND POTTORF, W.R., 1992. Systems tracts, seismic facies, Pand attribute analysis within as sequence stratigraphic framework — example from Offshore Louisiana Gulf Coast. *In:* Rhodes, E.G. and Moslow, T.F. (Eds.), *Marine clastic reservoirs*. Springer Verlag, New York, 21–38.

Manuscript received 1 October 1997